ELSEVIER

Ceramics International 25 (1999) 415–424

CERAMICS INTERNATIONAL

Early-stage sintering in a powder compact of polyhedral particles I. Models

Takayasu Ikegami

National Institute for Research in Inorganic Materials, 1-1, Namiki, Tsukuba-shi, Ibaraki, 305 Japan

Received 3 March 1998; accepted 19 May 1998

Abstract

An early-stage sintering model for polyhedral particles suggests combining the initial and intermediate stages. Kinetic equations based on the present model indicate a 1/3-power dependence of time for sintering controlled by volume diffusion. If sintering, on the other hand, is controlled by grain-boundary diffusion, the aforesaid combination decreases the power dependence of time from 1/4 to about 1/6 with sintering. Furthermore, the present model describes the variation of specific surface area by densification.

Keywords: A. Sintering; B. Microstructure-prefiring; C. Diffusion; Polyhedral

1. Introduction

Because solid-state sintering is a critical step in the processing of ceramics, numerous theoretical studies [1–8] have successively been devoted to its role in producing high-quality ceramics [9–11]. Sintering phenomena of the initial stage [1–5,12,13] were extensively analyzed at the beginning of history, especially in the field of powder metallurgy. Proposed theories successfully describe sintering of metal powders, but have caused serious controversies [14,15] on analyzing sintering data of ceramics. This may be attributed to anisotropic properties of ceramics, which essentially differ from isotropic properties of the reported model particles. The controversies concerned, however, gave us valid information to make a theory applicable to real sintering of ceramic powders, producing the present model of early stage sintering. An experimental application of the present model is examined elsewhere [16].

2. A review on sintering models of the initial stage

Initial-stage sintering has usually analyzed based on both the two spheres [1,3–5], or sphere-plate [2] (point contact) and wire-wire [17,18] (line contact) models. These studies produced the concepts of five sintering mechanisms. Fig. 1(A) shows a typical model of them as well as the diffusion paths (I to V) for the sintering mechanisms. As can be seen there, x is a contact radius; ρ is the minimum principle radius of curvature of the neck surface; 2 θ_s is defined as an equilibrium angle between the two tangents at the contacts of the neck surface with the two sphere surfaces; y is half a shrinkage between the adjacent centers of particles, and equals k_1x^2 for these usual models with the smoothly curved surfaces, where k_1 is a constant. Particles of metal are successfully described with spherical ones, and then reliable data have been accumulated. Ashby's sintering diagrams [19] well summarize essentials of those data.

Wulff construction [20], however, suggests that ceramic particles are polyhedral because of strong anisotropic properties of them in contrast with weak anisotropic ones of metal. Spheroidized particles [21,22] were then made under extreme conditions, such as very high temperature or mechanical polishing, to accord with the particle geometry of the usual models. These attempts, however, yielded negative results by faceting [22,23] of both spherical particles and their necks before initial-stage sintering. Recently, spherical, submicron powders have been made by applying various chemical processing techniques such as processing though monosized amorphous precipitates [24] or by the aid of impurities [25]. The experimental data with such a powder [24], however, resulted in unusually larger time exponents (> unity), suggesting unexpected mass transfer before or together with initial-stage sintering.

0272-8842/99/$20.00
PII: S0272-8842(98)00053-4

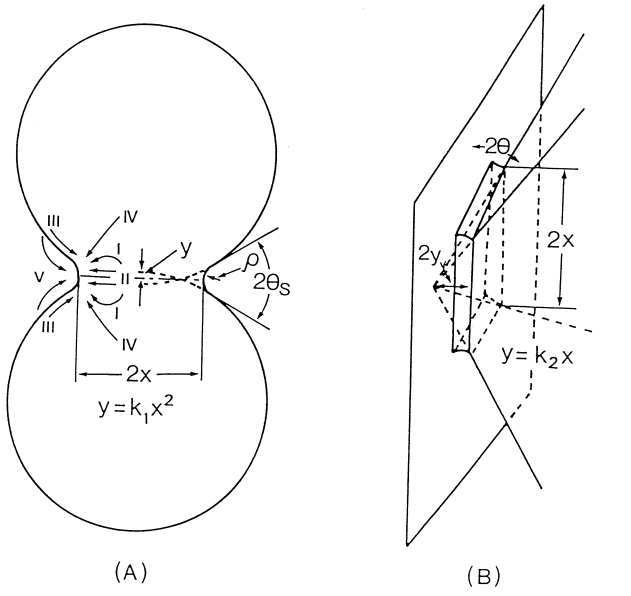

Fig. 1. Two typical models for the initial stage of sintering. (A) two-spheres and (B) Pyramid-plate. Path I is for volume diffusion, path II for grain-boundary diffusion, path III for surface diffusion, path IV for flow, and path V for evaporation-condensation..

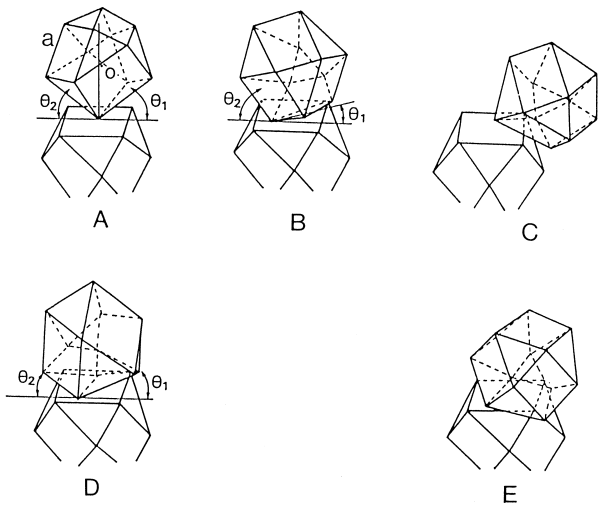

Fig. 2. Schematic contacts between polyhedra. A, point contact between a face and a corner with similar contact angels $\theta_1 \sim \theta_2$; B, point contact with large different θ values ($\theta_1 < \theta_2$); C, point contact between two edges of adjacent polyhedra; D, line contact; and E, face contact.

Some workers [26,27] already tried to model contacts between polyhedrons, that is, pyramid-plane and two pyramid contacts (a pyramid is equivalent to the corner of a polyhedron). All of them are point contacts. Fig. 1(B) shows a typical example, in which 2θ represents an angle between two faces of the particles forming the neck, and y equals k_2x, where k_2 is a constant. Three types [28] must be, however, considered for contacts between polyhedral particles, as shown in Fig. 2; A, a point contact with similar θ values ($\theta_1 = \&\theta_2$); B, a point contact with quite different θ values ($\theta_1 < \theta_2$), C, a point contact between two edges of adjacent particles; D, a line contact, and E, a face contact. Appendix A indicates that line contacts in them practically govern early-stage sintering of a powder compact.

Reported kinetic equations of sintering can be expressed with

$$\Delta L = \left(\frac{K}{R^P}\right)^{1/n} t^{1/n} \tag{1}$$

in general, ΔL a shrinkage of a powder compact; R, the average radius of particles; t, time; and K, n and p are constants. Table 1 shows the reported values of n and p, which depend on not only a neck geometry but also a width of diffusion field and a sintering mechanism. The history of kinetic equations led to rigid differential equations [29], from which a shrinkage rate slightly differs from that approximated by Johnson's equations [27]. This table, also, shows slight difference in the n values between Coble [5] and Johnson's [27] equations. These similarities support "qualitative" validity of Coble's equations. The n value in Table 1, on the other hand, is smaller for the usual models with smoothly curved surfaces by unity than for the sintering models with flat surfaces. This difference is attributed to the different relations between y and x, that is, y is proportional to x^2 for the former models, but to x for the latter models. Similar evaluation, on the other hand, was made for both a basic equation on mass flux and the width of diffusion fields regardless of the geometry of particles.

Volume elements [7,8,30] in a powder compact will be constrained to shrink uniformly. This condition suggests that a shrinkage between two adjacent particles depends directly not only on the neck geometry between them but also on packing irregularity in the powder compact. No quantitative information for such packing irregularity makes it difficult to estimate the initial conditions for the kinetic equations of sintering. This difficulty spoils 'quantitative' estimation of initial conditions for the aforesaid rigid differential equations, from which calculated data are ambiguous accordingly. Though Coble's equations are qualitative, the derivation of them is relatively simple. Then, the present kinetic equations were derived according to Coble's manner.

The distribution of not only particle sizes but also the θ values must be, also, considered at analyzing real initial-stage sintering of a powder compact. The starting θ value equals inevitably zero for the usual contact models with the smoothly curved surfaces. In this case, the former distribution has directly influence on densification of the powder compact, and Coble [31] derived sintering equations of the initial stage with a modified K value.

Table 1
The values of constants, p and n, for the reported shrinkage equations, $\Delta L = [\frac{K_o \gamma \Omega D}{kTR^p}]^{1/n} t^{1/n}$ K in Eq. (1) equals Ko$\gamma\Omega$/kT, where Ko is a constant dependent on the neck geometry, γ is the surface free energy, Ω is the atomic volume, D is the self-diffusion coefficient of atoms and kT has the usual meaning.

Model	Mechanism	p	n	Reference
Sphere-plate	Volume	3	2.5	Kuczynski [2]
Sphere-Sphere	Volume	3	2.5	Kingery and Berg [4]
Sphere-Sphere	Volume	3	2.0	Coble [5]
Sphere-Sphere (with groove)	Volume	3	2.04	Johnson [27]
160° cone on plate	Volume	3	3.0	Johnson and Cutler [13]
Pyramid-plate apex 120°	Volume	3	3.0	Bannister [26]
Sphere-sphere	Grain-boundary	4	3.0	Coble [5]
Sphere-sphere (with groove)	Grain-boundary	4	3.0	Johnson [27]
160° cone on plate	Grain-boundary	4	4.0	Johnson and Cutler [13]
Pyramid-plate apex 120°	Grain-boundary	4	4.0	Bannsiter [26]

The latter distribution, on the other hand, has influence on sintering of polyhedral particles. No study on the influence concerned led to the present study based on line contacts model of polyhedral particles, which produced a new concept, combining the initial and intermediate stages.

3. A sintering model for an assemblage of many polyhedral particles

Fig. 3 shows the schematic illustrations of the present neck model. The following assumptions were made to simplify the model.

1. As statistically estimated in Appendix B, all particles are polyhedrons equal in volume to a sphere of radius r, and the dihedral angle equals 120°.
2. The contact area between particles is negligibly small in the green compact.
3. The edge of each particle, which equals r in length, contacts the face of its neighbor; the cross section of a grown neck is accordingly rectangular.
4. The value 2 θ is defined as that in Fig. 1(B); θ_q ($q = 1,2$) is θ for neck q, $\theta_1 < \theta_2$ and then sum of $2\theta_1$ and $2\theta_2$ equals π minus the dihedral angle of the polyhedron. One-half the sum concerned equals 30°. The number of necks, dm, between θ_q and $\theta_q + \mathrm{d}\theta_q$ is directly proportional to $\mathrm{d}\theta_q$, but independent of the value of θ_q. The value M is the number of particles per unit weight, and n_c is the coordination number among the particles. The total number of necks is $n_cM/2$. Since the value of θ_q varies between θ to $\pi/6$, dm equals $6n_cM\mathrm{d}\theta_q/2\,\pi$.
5. The edge of a particle contacts at any position in the face of an adjacent particle at an equal frequency.
6. A slight difference between local and macroscopic shrinkage results in negligible rearrangement of the particles during sintering. If, then, $2Y$ is the initial length between the adjacent centers of particles, $\Delta L = y/Y$. The value of y equals one-half the length between O and C_1 in Fig. 3(A).
7. Negligible flux is tentatively assumed for the neck surface perpendicular to neck surfaces 1 or 2, in contrast with that for neck surfaces 1 or 2.
8. Thee mechanisms, that is, the flow mechanism, the surface diffusion mechanism, and the evaporation-condensation mechanism are negligible.

C_2 and C_2' in Fig. 3, as well as C_1, denote the edges of a particle. The grain boundary in this figure crosses neck surfaces 1 and 2 at points F and F′, respectively. The point at which the direction of the mass flux changes is designated O_1 in Fig. 3(A); atoms on the interface between F and O_1, x_1, diffuse to neck surface 1 with radius ρ_1, whereas those between F′ and O_1, x_2, diffuse to neck surface 2 with radius ρ_2. Fig. 3(B) also shows that the tangents of the neck surfaces at points A, A′, B and B′ can be replaced by lines AB, $A'C_1$ and $B'C_1$. Line AB crosses line $A'C_1$ at D and line $B'C_1$ at E; line C_1O is perpendicular to line AB.

The acute angle of the neck shown in Fig. 3 confines the grain boundary to the neck surface and induces appreciable neck growth, which is referred to as the initial stage of sintering. If, however, point A moves across edge C_2, or if point B moves across edge C_2', the value of θ_1 or θ_2 suddenly increases discontinuously. Appendix B suggests that once the neck surface has become blunted by sudden increase of θ_1, boundary motion becomes less inhibited, until grain growth is possible. Both the blunted neck surface by neck growth and beginning of grain growth fulfill the essences of Coble's criterion [6], which define the change from the initial to the intermediate stage. The rate of neck growth, however, increases with decreasing θ_q Appendix B, then, indicates that though a neck with a larger θ_q is still statistically in the initial stage of sintering, geometrical change occurs at a neck with a small θ_q value between the initial and the intermediate stage. Edge C_1 in Fig. 3 contacts the face C_2C_2' at an undefined

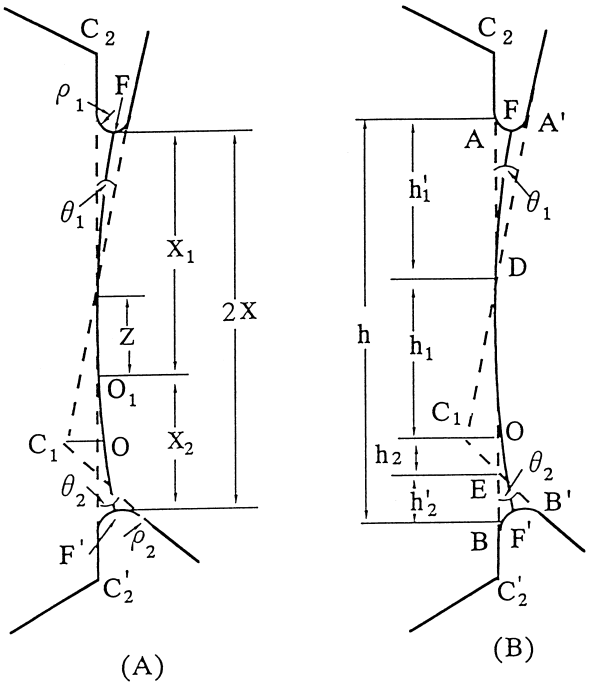

Fig. 3. A schematic model of initial stage sintering between a edge and a face of adjacent polyhedral particles. (A): atoms on the interface between O_1 and F, x_1, diffuse to neck 1 with radius ρ_1, and those on the interface between O_1 and F′, x_2, to neck 2 with radius ρ_2. z is an arbitrary length from O_1. (B): the geometry of a neck, in which edge, C_1, penetrates to the face C_2 and C_2'.

position. It is, then, difficult to relate length OC_1,$2y$, to a critical length OC_2 at which the aforesaid abrupt change of neck geometry just occurs.

Assumption 5, however, produces relations, $h_c = r/2$ and $2\theta_i = \tan^{-1}\ 8y/r$ in Appendix B, where h_c is an average of the critical lengths, and θ_i is the θ value for the neck with $OC_2 = h_c$. Necks with $\theta_i < \theta_1$ statistically represent the initial stage of sintering, and necks with $\theta_1 < \theta_i$ the intermediate stage. Using assumption 4, the number of necks in the initial stage is directly proportional to the range of θ between θ_i and 30°. The θ_i value, on the other hand, equals essentially zero for the green compact. Then, the number ratio, C_1, of necks of the initial stage remaining in a sintered compact to all the starting line contacts in the green compact can be given by the equation

$$C_I = \frac{30 - \theta_i}{30} \tag{2}$$

4. Shrinkage rates by volume diffusion and grain-boundary diffusion

z in Fig. 3(A) is defined as an arbitrary length from O_1 on the grain boundary, i.e. O_1F or O_1F'. The atomic flux [12], j_q ($q = 1,2$), can be expressed as

$$j_q = -\frac{Dq}{kT}\frac{d\mu_q}{dz} \tag{3}$$

where D_q is the self diffusion coefficient of the atoms, kT has the usual meaning, and $d\mu_q/dz$ represents a gradient of the chemical potential of the atoms. A powder compact shrinks by volume diffusion of the atoms as well as by grain-boundary diffusion of the atoms. If a neck satisfies assumptions 3 and 7, the width of the diffusion field can be estimated as $k_m\rho_q$ for volume diffusion and as δg for grain-boundary diffusion, where k_m is a constant, ρ_q is the radius of the neck surface q and δ_g is the thickness of the region of enhanced diffusion at the grain boundary. The total volume of the atoms [5] diffusing out from the grain boundary of length r during dt is given by $r(\delta_g j_g + k_m\rho_q j_v)$. The volume concerned equals the product of the shrinkage rate, $2dy_q/dt$, and the grain-boundary area, rz. From this equality and Eq. (3),

$$2z\frac{dy_q}{dt} = -\left\{\frac{k_g\delta_g D_g}{kT} + \frac{k_v\rho_q D_v}{kT}\right\}\frac{d\mu}{dz} \tag{4}$$

where k_g and k_v are constants containing a shape factor, D_g is the self-diffusion coefficient of the atoms for grain-boundary diffusion, and D_v is the self-diffusion coefficient of the atoms for volume diffusion. Assumption 7 estimates the values of ρ_q and ∞ for the two principal radii of curvature of neck surface q. ρ_q is very small in comparison with the principal radii of interfaces or particle surfaces in general. The reverse of ρ_q, therefore, governs the difference of the chemical potentials of atoms, $\Delta\mu$, between the neck surface and the interface or particle surface, and $\Delta\mu = -\gamma\Omega/\rho$, where γ is the surface free energy, and Ω is atomic volume.

Asymmetric neck geometry in Fig. 3 must induce a torque and a rotation of the particle with respect to the adjacent particle. The rearrangement of the particles [32] due to the torque and the rotation, however, causes inevitably simultaneous movement of a large number of particles around them in a powder compact. Such movement may be possible only by applying a force larger than one induced by the surface tension. The torque and the rotation concerned, then, are practically inhibited in fairly regular packing of particles of a powder compact. This inhibitory force against the torque or the rotation has influence on the value of $\Delta\mu$, which is modified as $\Delta\mu = k_t\gamma\Omega/\rho$, where k_t is a constant. Assumption 7 idealized extremely the flux of atoms to simplify the derivation of Eq. (4). The flux neglected by the assumption, however, must be taken into consideration for estimation of the actual mass flux, and thus requiring the correction, k_c, for the right hand side of Eq. (4). By using these estimations [5], integrating Eq. (4), with respect to z, from $z = 0$ to $z = x_q$ results in

$$\frac{dy_q}{dt} = \left\{\frac{k_g\delta_g D_g}{kT} + \frac{k_v\rho_q D_v}{kT}\right\}\frac{k_t k_c \Omega\gamma}{x_q^2\rho_q} \tag{5}$$

For simplification, two limiting cases are considered in the present study.

4.1. Grain-boundary diffusion is predominant

The second term on the right-hand side of Eq. (5) can be neglected, and

$$\frac{dy_q}{dt} = \frac{k_t k_c k_g \Omega\gamma\delta_g D_g}{kT\rho_q x_q^2} \tag{6}$$

Since a torque and a rotation of particles are inhibited as explained before, dy_1/dt equals dy_2/dt. From both this equality and Eq. (6),

$$\rho_1 x_1^2 = \rho_2 x_2^2 \tag{7}$$

From both Eq. (7) and $2x = x_1 + x_2$,

$$x_1 = \frac{2x}{1+\sqrt{\rho_1/\rho_2}} \tag{8}$$

$$x_2 = \frac{2x}{1+\sqrt{\rho_2/\rho_1}} \tag{8'}$$

Then, from Eqs. (6) through (8′),

$$\frac{dy}{dt} = \frac{k_t k_c k_g \Omega\gamma\delta_g D_g\left(\sqrt{\rho_1}+\sqrt{\rho_2}\right)^2}{4kT\rho_1\rho_2 x^2} \tag{9}$$

is derived. Eqs. (C5) and (C7) in Appendix C indicate that ρ_1 or ρ_2 is directly proportional to y for both the sintering mechanisms. Fig. 3, also, shows y and x directly proportional to a shrinkage, ΔL. The variables, y, x, ρ_1 and ρ_2 can, then, be replaced by ΔL with suitable constants. If the distribution of θ_q ($q = 1$ and 2) is very narrow (assumption 9) in contrast with assumption 4, and/or if dihedral angles of polyhedrons are very small (assumption 10) against assumption 1 (these assumptions are discussed in Appendix B), the transformation of necks occurs slightly from the initial to the intermediate stage due to sudden change in θ_I at the early stage of sintering. When, thus, a constant, K_g, is used instead of the product among elements, k_t, k_c, k_g, Ω, γ, δ_g, D_g, $1/kT$, and the aforesaid constants, Eq. (9) results in

$$\frac{d(\Delta L)}{dt} = \frac{K_g}{4\Delta L^3 r^4} \tag{10}$$

If sintering proceeds isothermally,

$$\Delta L_j^4 - \Delta L_j^4 = K_g(t_j - t_i)/r^4 \tag{10'}$$

where ΔL_j and ΔL_i are shrinkages at sintering time t_j and t_i. The aforesaid transformation, however, occurs successively in actual sintering of a powder compact, increasing markedly radii of curvature of the neck surfaces from ρ in the initial stage to r_p in the intermediate stage. The macroscopic driving force of such sintering, then, decreases more quickly than that estimated based on assumption 9 or assumption 10. It is difficult to deductively estimate a degree of the decrease concerned, but the constraint to shrink uniformly [7,8,30] is pointed above. This condition suggests that if few necks change their geometries between the initial and the intermediate stage, the macroscopic driving force (Appendix A) equals the integration of local driving forces for the initial stage from $\theta = \theta$ to $\pi/6$ as $2r\int_0^{\pi/6}(\gamma/\rho)(dm/d\theta)d\theta$. This constant integration range of θ produces a constant K_g. The aforesaid transformation, however, occurs considerably in usual sintering. The macroscopic driving force for the latter case equals the sum of $2r\int_{\theta i}^{\pi/6}(\gamma/\rho)(dm/d\theta)d\theta$ for the initial stage and $2r\int_0^{\theta i}(\gamma/r_p)(r/r_p)^4(dm/d\theta)d\theta$, for the intermediate stage. Then, the K_g value in Eq. (10) or (Eq. (10′) must be modified by the ratio of the latter driving force to the former one, as

$$\Delta L^3 d(\Delta L) = \frac{\left(\frac{r}{r_j}\right)^4\int_0^{\theta i}\frac{d\theta}{r_p} + \int_{\theta i}^{\pi/6}\frac{d\theta}{\rho}}{\int_0^{\pi/6}\frac{d\theta}{\rho}}\frac{Kgdt}{4r^4} \tag{11}$$

integration of Eq. (11) results in

$$\Delta L_j^{4+\xi} + \Delta L_i^{4=\xi} = K_g(t_j - t_i)/r^4 \tag{11'}$$

where r_j is the radius of a grown particle and ξ is an exponent correction due to the aforesaid transformation. A driving force of the intermediate stage is negligibly smaller than that of the initial stage because of a large inequality $d\theta/r_p < d\theta/\rho$. The numerator of the modified term in Eq. (11) indicates decreasing the integration range of θ between θ_i and $\pi/6$ for the local driving forces of the initial stage. The denominator, on the other hand, does the constant integration range. Then, the modified term decreases along with progressing sintering and the exponent of the ΔL term or reverse time exponent, n, in Eq. (11′) increases from 4 to about 6 (ξ changes from 0 to 2)

4.2. Volume diffusion is predominant

The first term on the right-hand side of Eq. (5) can be neglected in the case of volume diffusion, as

$$\frac{dy_q}{dt} = \frac{k_t k_c k_v \gamma\Omega D_q}{kTx_q^2} \tag{12}$$

This equation has no term about ρ. This is because the increase of ρ results in both decreased driving force, γ/ρ,

and increased width of the diffusion field, $k_m\rho$, for volume diffusion. The product of the driving force and the width of diffusion field equals k_m, which has no explicit element on the curvature of a neck surface. According to Coble's model for the initial stage, the k_m value is proportional to angle ADA′ ($=\pi-2\theta_q$) shown in Fig. 3(B). Both the θ_i and θ'_i value are much smaller than π. The sudden change of the neck geometry, thereby, results in a relatively small decrease in angle ADA′ from ($\pi-2\theta_i$) to ($\pi-2\theta'_i$) in compared with appreciable increase of θ from θ_i to θ'_i. The k_m value, thus, changes slightly in contrast with the marked variation of ρ.

Both Eq. (12) and the equality between dy_1/dt and dy_2/dt give another equality,

$$x_1 = x_2 \tag{13}$$

x_q is directly proportional to r or Y for a given shrinkage ΔL, and $x_q = k_n r\ \Delta L$, where k_n is a constant. The statistical calculation of Eq. (12) under assumption 6, $\Delta L = y/Y$, results in

$$\frac{d(\Delta L)}{dt} = \frac{K_v}{3\Delta L^2 r^3} \tag{14}$$

and, if sintering proceeds isothermally,

$$\Delta L_j^3 - \Delta L_i^3 = K_v(t_j - t_i)/r^3 \tag{14′}$$

where K_v is used instead of ($k_t k_c k_v k_n{}^2 \Omega\gamma D_v/kT$). Some of the elements in this bracket slightly change during sintering, and the rest are constants. The values of K_v and n ($\sim$3) in Eq. (14′) are then practically unchangeable.

5. Decrease of surface area during sintering

The growth of necks 1 and 2 induces both decreased particle surface area ($=-2hr$) and increased neck surface area [$=\{\rho_1(\pi-2\theta_1)+\rho_2(\pi-2\theta_2\}r$]. Furthermore, growth of the necks perpendicular to neck 1 or 2 also induces both decreased (&10yh) particle surface areas and increased (&4yh) neck surface areas. The net change in surface area, s_i, is given by

$$s_i \approx (2r+6y)h - \{\rho_1(\pi-2\theta_1)+\rho_2(\pi-2\theta)_2)\}r \tag{15}$$

The h ($=h_1+h_2+h_1'+h_2'$) value was calculated in Appendix C, and shown in Fig. 4 with the solid line, a, for the volume diffusion mechanism, and with the long dashed line, b, for the grain-boundary diffusion mechanism. Both the slightly curved lines indicate that h nearly equals $2(h_1+h_2)$ for the two mechanisms regardless of the θ_1 value, and h is estimated as equal to

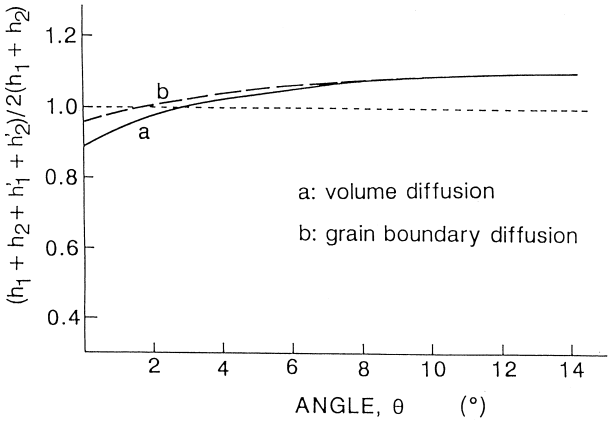

Fig. 4. Slight influence of angle θ_1 on ratio $(h_1+h_2+h_1'+h_2')/2(h_1+h_2)$ both for the volume diffusion mechanism, line a, and for the grain-boundary diffusion mechanism, line b.

$2(h_1+h_2)$. The right-hand side of Eq. (15), readjusted with both Eq. (C1) through Eq. (C5) and equalities, $h=2(h_1+h_2)$ and $\theta_1+\theta_2=30°$, has only two variables, y and θ_1.

The pore surface area per neck [33], s_m, in the intermediate sintering stage is given by

$$s_m = k_{s1}r_p^2 - k_{s2}r_p r \tag{16}$$

where k_{s1} and k_{s2} are constants. If only a packing structure governs the shape of grains, sintering extends the grain boundary areas but reduces the grain surface areas. This indicates appreciable change in the shape of grains, that is, in the shape factor, k_c, related to the total area (surface area + grain-boundary area) characteristics of the grains. The changing of the shape concerned means deviating from the stable shape suggested by the Wulff construction [20]. The actual shape of grains, therefore, must depend on their intrinsic properties as well as the packing structure, and the values of k_{s1} and k_{s2} are modified so that the k_c value remains constant regardless of degree of densification. The number of necks between θ and $\theta+d\theta$ decreases from dm to dm' during intermediate-stage sintering. dm' equals $(r/r_j)^3$ dm. From Eq. (15) and Eq. (16), S_p for a sintered compact is given by

$$S_p = M(1-\frac{3\theta_i}{\pi})k_c r^2 - \frac{3n_c M}{\pi}\int_{\theta i}^{\pi/6} S_i d\theta + \frac{3n_c M}{\pi}\int_0^{\theta_i}\left(\frac{r}{r_j}\right)^3 s_m d\theta \tag{17}$$

where $k_c r^2 M$ naturally equals the specific surface area of a powder. The first and the second terms in the right hand side of this equation estimate the sum of the total areas (surface areas plus interfacial areas) of particles and the total of the s_i values in the initial stage, respectively. The last term in it concerns to the total of the pore surface areas, S_m, in the intermediate stage.

6. Discussion

Since a ceramic powder is crystalline in general, polyhedral particles are suggested by Wulff construction [20] instead of spherical ones. The validity of assumptions 1 and 3 is evaluated in Appendix B. Assumptions 4 and 5 hold for fairly random packing of particles, which must practically be realized in a powder compact of equiaxed particles due to their slightly oriented packing. Assumption 6 accords with the aforesaid requirement to shrink uniformly. The derivation of Eq. (4) needs very idealized assumption 7, and then the correction factor, k_c, is introduced to estimate the actual mass flux. The validity of assumptions 2 and 8 naturally depends on both the packing geometry and properties of a powder which must be effectively controlled by powder processing technology.

The present model differs sharply from the other models in regard to the initial angles, θ_1 or θ_s, between neighboring faces: The former model describes the sintering of necks with dispersed θ_1 values, which induce an intermediate stage of sintering along with the initial sintering stage, even in the range $\Delta L = 0\%$ to approximately 5%; this combination of the initial stage and the intermediate stages induces a variable kinetic exponent for shrinkage if sintering is controlled by grain-boundary diffusion. The other models, on the other hand, implicitly assume equal θ values, and every neck changes simultaneously its geometry from the initial to the intermediate stage. Constant kinetic exponents have been derived consequently. Naturally, if some of them, such as the pyramid-plate [Fig. 1(B)] and the cone-plate are modified to dispersed the θ values, combining the initial and the intermediate stages should occur. The initial θ value, on the other hand, equals essentially zero for the usual sintering systems of $y = k_1 x^2$ such as sphere-sphere [Fig. 1(A)], sphere-plate, or wire-wire contacts.

Combining the initial- and intermediate-sintering stages should occur even for spherical particles in three cases, for three packing geometries of particles within a green compact: (1) dispersed contact areas between the particles, (2) heterogeneous packing of particles, and (3) dispersed particle sizes. It is, however, difficult to estimate both the distribution of the contact areas and the packing structure of the particles in the green compact, a difficulty that limits valid discussion for the first two cases. Coble [31] analyzed sintering among particles with dispersed radii, but his work concerned only the initial stage in the limited variation of ΔL. If, however, dispersed radii of the particles are measured, kinetic equations for the combined initial and intermediate sintering stages can be derived according to the method presently proposed.

Driving forces, γ/ρ, for the initial stage are very larger than those γ/r_p for the intermediate stage because of $\rho < r_p$ in general. The constraint [7,8,30], stated in Section 2, suggests that even if major necks in the sintered compact are not in the initial sintering stage, the driving forces of the initial stage effectively govern the sintering of necks with intermediate stage geometry. The ρ value is dependent on both ΔL and θ but also depends somewhat on r and r_p. The effective driving forces thus are negligibly influenced by not only grain size distribution but also pore size (the packing densities of the micro-regions [33]). This negligible influence supports assumptions 1 and 3 (equal-sized particles), as well as the implicit assumption that when few new particle-to-particle contacts occur during sintering, the packing structure of the green compact has no measurable influence on the sintering rate, ΔL, in the initial stage. The present kinetic equations consequently have no explicit term for the aforesaid distributions.

7. Summary

The review on sintering theories for the initial stage classifies accumulated knowledge on sintering phenomena into two groups, that is, reliable and unreliable. A great consensus has been achieved about a driving force and five sintering mechanisms. Serious controversies, on the other hand, have been occasioned for reported kinetic equations due to large difference between the simple models of idealized necks in the theoretical studies and complex geometry of real necks in a powder compact. The present study, however, suggests a possibility that such complexity can be simplified with the requirement concerned to shrink uniformly in a powder compact. The requirement and dispersed dihedral angles between faces of particles lead combining the initial and intermediate stages of sintering, which considerably decreases the power dependence of time during sintering controlled by grain-boundary diffusion mechanism.

Appendix A

The minimum circumference of a neck, L_m, approximates to $4\pi\sqrt{yr}$ for the usual model of the point contact [3–5,9] between two-spheres, $2r$ on the average for the present line contact model between polyhedra and about $30y$ for a Bannister's model [26] of the point contact between polyhedra with the dihedral angle of 150°. The product of γ/ρ and L_m, F_d, is proportional to the local driving force of sintering at the neck concerned. With the relations $y = \rho$ and $\Delta L = y/r$, the F_d value approximates to $4\pi\gamma\sqrt{\Delta L}$ for the usual models, $2\gamma/\Delta L$ on the average for the present model, and about 30 γ for Bannister's model. The F_d value is inversely proportional to ΔL for the present model and the square root of ΔL for the usual model. The F_d value for Bannister's model is a constant regardless of the ΔL

value. Thus, the present model produces the markedly large F_d value at the beginning of sintering from $\Delta L=0$ to 2.5% in the aforesaid three models, especially at a lower ΔL value. Bannister's model, on the other hand, has the smallest F_d value in the range from $\Delta L=0$ to 7% in those models.

A recent packing simulation [28] with polyhedra revealed the three kinds of contacts shown in Fig. 2: the point contacts type, A to C: the line contact, type D: and the face, contact type E. The relative frequencies among them were 60% for the line contacts and about 20% for not only the sum of the point contacts, types A to C, but also the face contacts. The necks of B type point contacts quickly grow along by edges, and transform to necks similar to the line-contact necks. Such transformation means practical increase of line contacts from 60% during sintering.

Increase of a neck radius results in not only (1) reducing the driving force for sintering, but also (2) increasing lengths between diffusion sources and diffusion sinks. Furthermore, a shrinkage rate decreases due to increasing the contact area of the neck even if an amount of mass transfer per unit time is the same (the amount concerned equals the product of the shrinkage rate and the contact area of the neck). This assumption is inconsistent with phenomena (1) and (2), which indicate that neck growth decreases the amount of mass transfer. The actual shrinkage rate is, therefore, decreased by neck growth more quickly than that estimated under the assumption mentioned just earlier. These evaluations indicate that in the initial stage of sintering, face contacts slightly contribute to shrinkage between particles, and particles joined by the face contacts consequently behave like large particles in a powder compact. The face contacts, thus, rule out from counting the necks effective in shrinkage between particles, that is, densification of a powder compact in the initial stage.

This appendix evaluates the four factors, that is, the F_d value, the relative frequencies among the contacts, the transformation from the necks of B type point contacts to those of the line contacts, and the negligible effect of the face contacts on shrinkage of a powder compact in the initial stage. All these evaluations suggest that the line contacts predominantly govern early-stage sintering in the assemblage of polyhedral particles.

Appendix B

We assume that all particles are tetradekahedrons, which have 36 edges of length l_p. The dihedral angle is 125°16′ for 24 edges and 109°28′ for 12 edges. The average angle of them equals 120° $\{=(125°16'\times24+109°28'\times12)/36\}$. When a sphere of radius r equals the polyhedron in volume, $8\sqrt{2}l_p^3=4\pi r^3/3$, and $r=1.393l_p$. The polyhedron has 14 faces, of which the average area equals $1.9131_p{}^2$ $\{=(2.598\times81_p{}^2+61_p{}^2)/14\}$. The face with the average area is described with a square of edge length r' (assumption 3), $r'=1.3831p$. The similar values between r and r' means that a face of the polyhedron can be described with the square of length r at the statistically average point of view.

Fig. 5(A) shows edges a to c, which just change their geometries from the initial to the intermediate stage. Point O_a for edge a or point O_c for edge c has the same meaning as point O defined in Fig. 3. Edge a in them has the smallest θ_1 value and the largest θ_2 value, which respectively approximate to zero and 30° because of $2y \ll$ length C_2O_a. Length $C_2'O_a$, then, approximates to $4y\sqrt{3}$. Edge c, on the other hand, has the largest θ_1 $(=15°)$ and the smallest $\theta_2(=15°)$ value in those edges. Length O_cC_2', thereby, equals $r-4y\sqrt{3}$. Since y is negligibly smaller than r, length C_2O varies practically in the range between 0 to r. Assumption 5, then, roughly defines an average, $h_c=r/2$, for length C_2O. Fig. 5(B) defines the angle, θ_i, for the neck with h_c as $\tan^{-1}8y/r$. Necks with $\theta_1>\theta_i$ are statistically still in the initial stage as shown in Fig. 5(B), but necks with $\theta_1<\theta_i$ have changed in shape from the initial to the intermediate stage. Increase of the θ_i value with progress of sintering means that of necks in number in the intermediate stage.

Coble [6] indicated that the intermediate stage begins, after the interparticle contact area becomes to a critical area, that is, 0.2 of the cross-sectional area of spherical particles $\{s_c=0.63r^2\}$. The s_c value of the present model, on the other hand, equals $r(h_c+h_2+h_2')$, which increases from 0.16 of the cross-section area of polyhedral particles with increasing a shrinkage, ΔL, as 0.16, 0.17, 0.18 and 0.22 for $\Delta L=0.5$, 1.0, 2.0 and 4.0%, respectively. Migration of a neck must become easy with increasing its cross-sectional area because of

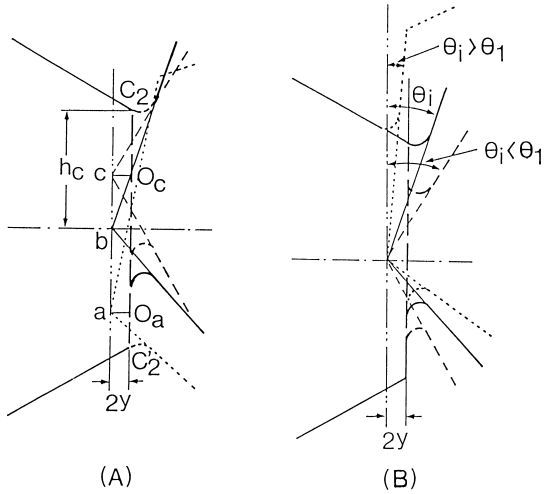

Fig. 5. Two schematic models of neck geometries at a given ΔL; (A) necks of which is the geometry just changes from the initial to intermediate stage. θ_i is θ_1 of such a neck; (B) a neck with $\theta_i<\theta_1$, in the initials stage, and a neck with $\theta_1<\theta_i$ in the intermediate stage.

increasing its bluntness. The viewpoint of the s_c value, therefore, suggests that migration of the critical neck is more difficult between $\Delta L=\theta$ to 2.8% for the present model than for the two-sphere model.

The sudden geometrical change of a neck brings about the change of the θ_1 value from θ_i in the initial stage to θ'_i for the intermediate stage. The average value, θ_c, equals 30° for four angles around the necks concerned, that is, θ'_i, θ_2 and the angles of the neck surfaces perpendicular to the neck surfaces 1 and 2. Coble model [6], on the other hand, defines the critical angle, $\theta'_c=26°57'$, at which the intermediate stage begins. A neck with a larger θ_c or θ'_c value means more blunted, which suggests that migration of the critical neck is easier for the present model than for the usual model. This examination is in contrast with the aforesaid evaluation based on the s_c value. These inconsistent evaluations suggest similar mobilities of the critical necks between the present and the usual model.

Assumption 9 means inappreciable existence of necks with peculiarly small θ_1 values, according with rather simultaneous change of neck geometries from the initial to the intermediate stage. A polyhedron satisfying assumption 10, on the other hand, has a small number of faces, of which the area is estimated as r'^2. The r' value is consequently larger than the r value. From the relations of $2\theta_i=\tan^{-1}8y/r'$ and $\Delta L=y/Y$, the θ_i value for a given ΔL value is smaller for the polyhedron with the larger r' value than for the present polyhedron. The sum of $2\theta_1$ and $2\theta_2$, on the other hand, equals $\pi/2$ minus the dihedral angle of the polyhedron, and then increases with decreasing the dihedral angle concerned. Eq. (2) with these estimations—a small θ_i value and the large sum of $2\theta_1$ and $2\theta_2$—gives a larger C_I value for assumption 10 than that for assumption 4. Consequently neck geometries of cubic or tetrahedral particles, satisfying assumption 10, slightly change from the initial to the intermediate stage in the early-stage sintering.

Appendix C

Fig. 3(B) shows the relation

$$2y = h_q tan2\theta_q \tag{C1}$$

Several areas can also be estimated as

$$area\ C_1OD = 2y^2\ \cot\ 2\theta_1 \tag{C2}$$

$$area\ C_1OE = 2y^2\ \cot\ 2\theta_2 \tag{C2'}$$

$$s_q \approx \frac{1}{2}\rho_q^2 \cot\ \theta_q(1-\sin\theta_q),\ (q=1\ and\ 2) \tag{C3}$$

where s_i equals area ADF and S_2 equals area BEF′. The total mass of atoms that diffuse to neck surface q equals the product of $2S_q$ and neck length, r. It is natural, then, that

$$S_1 + S_2 = y^2(\cot\ 2\theta_1 + \cot\ 2\theta_2) \tag{C4}$$

because of an equality between area ADA′ + area BEB′ and area C_1OD + area C_1OE.

If the volume diffusion mechanism predominates over sintering, $s_1=s_2$ is derive from Eq. (13). Combining Eqs. (C2), (C2) and (C3) results in Eq. (C5).

$$\rho_q = y\sqrt{\frac{(\cot\ 2\theta_1\ +\ \cot\ 2\theta_2)}{\cot\ \theta_q(1\ -\ \sin\ \theta_q)}} \tag{C5}$$

If the θ_1 and y values are given, length AD, $h'_1=\rho_1\cot\theta_1$, or length BE, $h'_2=\rho_2\cot\theta_2$, can be calculated easily with Eq. (C5). The solid line, a, in Fig. 4 shows the $(h_1+h_2+h_1'+h_2')/2(h_1+h_2)$ value calculated with the estimated h_1' and h_2' values and Eq. (C1). If, on the other hand, the grain-boundary diffusion mechanism predominates over sintering, dy/dt depends on three variables, ρ_1, ρ_2 and x as predicted from Eq. (9), and direct estimation on the h'_q value is difficult. The ratio s_1/s_2, however, equals that between amounts of mass transfer to neck surfaces 1 and 2 ($=x_1/x_2$). Combining the relation $s_1/s_2 = x_1/x_2$ with Eq. (8) and (C3) results in

$$\rho_2 = k_n\rho_1 \tag{C6}$$

or

$$\frac{h'_2}{h'_1} = k_n\frac{\cot\ \theta_2}{\cot\ \theta_1} \tag{C6'}$$

where

$$k_n = \sqrt[5]{\cot\ \theta_1(1\ -\ \sin\theta_1)/\{\cot\ \theta_2(1\ -\ \sin\ \theta_2)\}}$$

From Eqs. (C3)and (C6),

$$\rho_1 = y\sqrt{\frac{2(\cot\ 2\theta_1\ +\ \cot\ 2\theta_2)}{\cot\ \theta_1(1\ -\ \sin\ \theta_1) + k_n^2\cot\ \theta_2(1\ -\ \sin\ \theta_2)}} \tag{C7}$$

The long dashed line, b, in Fig. 4 was obtained with Eqs. (C1), (C6) through (C7) and the relation $h'_q=\rho_q\cot\theta_q$.

References

[1] J. Frenkel, Viscous flow of crystalline bodies under the action of surface tension, J. Phys. (USSR) 9 (5) (1945) 385–391.
[2] G.C. Kuczynski, Self-diffusion in sintering of metallic particles, Trans. AIME 185 (2) (1948) 169–178.

[3] C. Herring, Effect of change of scale on sintering phenomena, J. Appl. Phys. 21 (4) (1950) 301–303.
[4] W.D. Kingery, M. Berg, Study of the initial stages of sintering solids by viscous flow, evaporation–condensation, and self-diffusion, J. Appl. Phys. 26 (10) (1955) 1205–1212.
[5] R.L. Coble, Initial sintering of alumina and hematite, J. Am. Ceram. Soc. 41 (2) (1958) 55–62.
[6] R.L. Coble, Sintering crystalline solids: I and II, J. Appl. Phys. 32 (5) (1961) 787–799.
[7] D.L. Johnson, A general model for the intermediate stage of sintering, J. Am. Ceram. Soc. 53 (10) (1970) 574–577.
[8] A.G. Evans, Consideration of inhomogeneity effects in sintering, J. Am. Ceram Soc. 65 (10) (1982) 497–501.
[9] W.H. Rhodes, Agglomerate and particle size effects on sintering yttria-stabilized zirconia, J. Am. Ceram. Soc. 64 (11) (1981) 19–22.
[10] C. Greskovich, J.P. Chernoch, Polycrystalline ceramic lasers, J. Appl. Phys. 44 (10) (1973) 4599–4606.
[11] C. Greskovich, J.H. Rosolowski, Sintering of covalent solids, J. Am. Ceram Soc. 59 (7-8) (1976) 336–343.
[12] C. Herring, Surface tension as a motivation for sintering, in: T.E. Kingston (Ed.), The Physics of Powder Metallurgy, McGraw-Hill, New York, 1951, chapter 8.
[13] D.L. Johnson, I.B. Cutler, Diffusion sintering: I and II, Initial stage sintering models and their application to shrinkage of powder compacts, J. Am. Ceram Soc. 46 (11) (1963) 541–550.
[14] H.E. Exner, G. Petzow, A critical evaluation of shrinkage equations, in: G.C. Kuczynski (Ed.), Mat. Sci, Res. vol. 13, Plenum Press, New York, 1980, pp. 107–120.
[15] J.M. Dynys, R.I. Coble, W.D. Coblenz, R.M. Cannon, in: G.C. Kuczynski (Ed.), Mat. Sci, Res. Vol. 13, Plenum Press, New York 1980, pp. 391–404.
[16] T. Ikegami, Y. Kitami, M. Tsutsumi, Early-stage sintering in a powder compact of polyhedral particles: II. Experimental analysis with a highly sinterable Al_2O_3 powder, Ceramics International, submitted for publication.
[17] R.M. German, Z.A. Munir, Identification of the initials stage sintering mechanism using aligned wires, J. Mater. Sci. 11 (1976) 71–77.
[18] A.L. Pranatis, L. Seigle, Sintering of wire compacts, in: W. Leszynski (Ed.), Powder Metallurgy, Interscience, New York, 1961, pp. 53–73.
[19] M.F. Ashby, A first report on sintering diagrams, Acta Metall. 22 (3) (1974) 275–289.
[20] G. Wulff, Zur Frage der Geschwindigkeit des Wachstums und der Aufloesung der Kristallflaehen (about the velocity of growth and dissolution of crystal faces), Z. Kristallogr. 34 (1901) 449–530.
[21] A. Asaga, K. Hamano, Initial sintering kinetic of compacts of spherical particles, Yogyo-Kyokai-Shi 83 (3) (1975) 146–147.
[22] P. Kumar, D.E. Johnson, Sintering of CoO: I, initial stage, J. Am. Ceram Soc. 57 (2) (1974) 62–64.
[23] L. Navias, Sintering experiments on sapphire spheres, J. Am. Ceram Soc. 39 (4) (1956) 141–145.
[24] E.A. Barringer, R. Brook, H.K. Bowen, The sintering of monodispersed TiO_2, in: G.C. Kuczynski, A.E. Miller, and G.A. Sargent (Eds.), Sintering and Heterogeneous Catalysts, Plenum Press, New York, 1984, pp. 1–21.
[25] D.J. Sordelet, M. Atkinc, Sintering of monosized spherical yttria powders, J. Am. Ceram Soc. 71 (12) (1988) 1148–1153.
[26] M.J. Bannister, Shape sensitivity of initial sintering equations, J. Am. Ceram Soc. 51 (10) (1968) 548–553.
[27] D.L. Johnson, New method of obtaining volume, grain-boundary, and surface diffusion coefficients from sintering data, J. Appl. Phys. 40 (1) (1969) 192–200.
[28] T. Ikegami, Contacts and coordination numbers in a compact of polyhedral particles, J. Am. Ceram Soc. 79 (1) (1996) 148–152.
[29] R.L. Eadie, D.S. Wilkinson, G.C. Weatherley, The rate of shrinkage during the initial stage of sintering, Acta Metall. 22 (10) (1974) 1185–1195.
[30] T. Ikegami, K. Kotani, K. Eguchi, Some roles of MgO and TiO_2 in densification of a sinterable alumina, J. Am. Ceram Soc. 70 (12) (1987) 885–890.
[31] R.L. Coble, Effects of particle-size distribution in initial-stage sintering, J. Am. Ceram Soc. 56 (9) (1973) 461–466.
[32] T. Ikegami, Theoretical description of a two-dimensional compaction process of cylinders, J. Am. Ceram Soc. 79 (1) (1996) 153–160.
[33] T. Ikegami, Y. Moriyoshi, Intermediate-stage sintering of a homogeneously packed compact, J. Am. Ceram Soc. 67 (3) (1984) 174–178.